

Efficient Design of Hardware-Enabled Reservoir Computing in FPGAs*

Bogdan Penkovsky, Laurent Larger, and Daniel Brunner
*FEMTO-ST / Optics Dept., UMR CNRS 6174, Univ. Bourgogne Franche-Comté,
 15B avenue des Montboucons, 25030 Besançon Cedex, France*
 (Dated: October 3, 2018)

In this work, we propose a new approach towards the efficient optimization and implementation of reservoir computing hardware reducing the required domain expert knowledge and optimization effort. First, we adapt the reservoir input mask to the structure of the data via linear autoencoders. We therefore incorporate the advantages of dimensionality reduction and dimensionality expansion achieved by conventional algorithmically efficient linear algebra procedures of principal component analysis. Second, we employ evolutionary-inspired genetic algorithm techniques resulting in a highly efficient optimization of reservoir dynamics with dramatically reduced number of evaluations comparing to exhaustive search. We illustrate the method on the so-called single-node reservoir computing architecture, especially suitable for implementation in ultrahigh-speed hardware. The combination of both methods and the resulting reduction of time required for performance optimization of a hardware system establish a strategy towards machine learning hardware capable of self-adaption to optimally solve specific problems. We confirm the validity of those principles building reservoir computing hardware based on a field-programmable gate array.

I. INTRODUCTION

Machine learning (ML) development has drastically progressed during the last decade. To only name a few examples, now machines can accurately describe images [1], identify and recognize faces [2], recognize speech [3] and compose music [4, 5]. In 2017, AlphaGo Zero and AlphaZero with no prior domain knowledge have beaten the best human and machine players both in Go [6] and chess [7] games. These all are challenges which, until recently, were thought to remain reserved for the human intelligence only.

However, the efficiency of current ML methods is restricted by hardware, which in its turn is fundamentally limited by the minimal transistor size. Another potential issue is related to the fact the vast majority of ML hardware rely only on a single design: the Turing-von Neumann architecture. That results in the second, conceptual limitation: our machines are constrained by their implementation's design, and that design is mostly one. A viable way to circumvent present limitations is by shifting the design paradigm away from Turing-von Neumann architectures. This shift may also give insight into questions related to self-adapting hardware.

In this paper, we demonstrate the implementation of a single-node reservoir computer (RC) [8] in field-programmable gate array (FPGA) hardware. Hardware-implementation of such time-delay reservoirs (TDRs) is particularly resource efficient. They mostly consist of a first-in first-out (FIFO) memory combined with a single nonlinear dynamical node. Yet even such simple systems have a parameter space with dimensionality too-high for exhaustive parameter optimization to be realistic. We propose genetic algorithms (GAs) for enabling our TDR-hardware to quickly optimize its dynamical properties,

achieving a reduction by 2-3 orders of magnitude in optimization effort. Thanks to such improvement and the ease of hardware-implementation of a GA, future systems will be able to adjust to unforeseen changes in data [9]. Addressing potential bottlenecks in the input-interface, we merge the system's input weight-matrix with auto-encoders realizing principle component analysis. With this approach we achieve data-injection efficiency increase by a factor of 1.8. As a proof-of-concept, we prototype the self-adapting system in simulation, evaluate it on a speech recognition benchmark, and verify the validity of the approach using an FPGA. The results achieved by FPGA-based RC with limited bit resolution closely match those obtained in simulations with noise, confirming our strategy for future design of TDR-systems based on physical nonlinear substrates.

A. Reservoir computing. Single-node approach

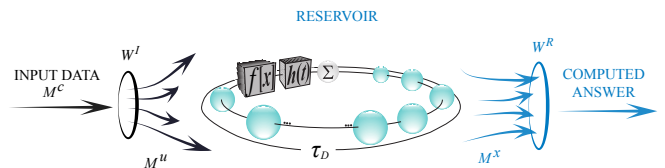


Figure 1. **Single-node reservoir computing architecture.** The three core components are: input masking, reservoir transformation, and linear readout. First, the input data M^c are masked by multiplying the mask W^I , then the masked input M^u is transformed by reservoir's nonlinear delay dynamics. Finally, the answer is obtained by multiplying the readout W^R and the reservoir's state M^x .

* {bogdan.penkovskyi,laurent.larger,daniel.brunner}@femto-st.fr

Reservoir computing (RC) first appeared as a modification to recurrent neural networks (RNNs) training and

was proposed independently in [10–12]. Due to the retained internal state, RNNs are also known as “deep” neural networks. Because of the practically infinite number of hidden layers, gradient-based training of RNNs often suffers from exploding or vanishing gradients. RC solved the problem of RNN training by applying the principle of a random mapping. Reservoir acts as a spatiotemporal kernel mapping the low-dimensional input information onto a higher-dimensional state space, where this information is expected to become linearly separable [13]. Therefore, a linear readout interpreting *transient* dynamics in the high-dimensional network’s state should be sufficient to interpret that information. As a consequence, instead of adapting the whole recurrent network, only the linear readout layer is trained in RC.

The RC approach achieves multiple objectives: (1) the training procedure is fast, and (2) is guaranteed to converge using conventional linear algebra techniques, and crucially for the development of novel computing systems, (3) the fixed nonlinear part of the network can practically be delegated to low-level hardware, i.e. physically existing dynamical systems, not limited to digital electronics. Reservoir computing is a computation paradigm that potentially addresses the issues of inherently fast and energy-efficient hardware. This is mainly due to its support of information processing directly on the very hardware level. Several experimental implementations of RC hardware are known: using digital-analog electronics [8, 14], electro-optical and all-optical systems [15–18], and spintronic nanoscillators [19]. Both numerical and experimental RC systems often beat state-of-the-art in speed (such as in speech recognition task [20]) and accuracy (e.g. time series prediction [21]).

The single-node RC is a technique that uses a complex nonlinear delayed-feedback system as a dynamical reservoir [22]. This delay system is a recurrent network which retains its internal state as the state of the delay line. The single-node approach to RC takes advantage of delay dynamics, which has a high-dimensional, mathematically speaking even infinite-dimensional phase space, and can be interpreted as a virtual network [8, 23]. Single-node RC is frequently implemented in hardware as it is a technologically efficient way to construct a nonlinear reservoir network. The benefit of the method is the ability to reduce the physical neural network’s size to a single nonlinear unit, thereby resulting in a smaller number of dynamical parameters to control. Moreover, the single-node RC architecture is especially suitable for ultrahigh-speed photonic hardware implementations [20]. Numerous other demonstrators have validated the single-node RC approach showing autonomous RCs [24] and variety of hardware architectural and training modifications [25–27].

The present work is two-fold. First, it addresses the problem of *hyperparameters* [28] optimization in RC, which was also discussed in [29]. However, we apply genetic algorithms as the optimization strategy and validate the method on actual hardware, addressing the pos-

sibility of real-world hardware design. In [30, 31] genetic algorithms were also applied, however to a different RC architecture (echo state network) and with no attempt at hardware implementation, while in this work we consider the single-node architecture. Second, an optimal input matrix is constructed by stripping input data of trivial information. The combination of both methods, genetic algorithm and *autoencoder*, is applied for the first time to hardware-implemented RC.

A general single-node RC architecture is schematically represented in Fig. 1. Input information M^c is masked by the input mask W^I and then, mapped as M^u on a high-dimensional state space of a delay reservoir. Then, the reservoir’s nonlinear response creates a state matrix M^x . The final answer is obtained by a linear readout, i.e. by multiplying matrix W^R . An introduction to the single-node RC can be found in [8, 20, 32].

B. Input streamlining

In [33] it was suggested that information processing in the brain (e.g. in the primary visual cortex) is performed in three stages: first, input projection into principal feature dimensions, second, redundant information filtering, and finally third, higher-level information processing. Motivated by that strategy, we propose automatic feature weighting via redundant information filtering, to enhance the conventional random masking of RC. That is achieved by principal component analysis (PCA), a technique that constructs linear combinations of input features.

First, we apply PCA to remove the dimensions with the lowest variance, i.e. to compress the input data. That allows us to focus on the input data’s most relevant structure. Then, an inverse to compression operation, dimensionality expansion, is employed to restore the shape of the inputs. These two linear operators, compression and expansion [34], partially remove irrelevant feature information, such as noise. Therefore, PCA plays the role of an *autoencoder* (autoassociative neural network), a network utilized to learn efficient data coding. In practice, application of PCA-based compression-decompression is very similar to the application of an autoassociative neural network with a single hidden layer [35]. Finally, random masking conventional to RC is performed in order to map the information onto a higher dimensional state space of the reservoir.

C. Self-adapting reservoir dynamics

Due to the simplified training step in RC, the main action in system performance optimization is dynamical system parameters exploration. While the single-node RC method’s complexity is much reduced, this can still be a substantial bottleneck for real-world applications since each problem may require a different set of dy-

namical parameters. For instance, a set of optimized speech recognition system parameters is potentially different from that of handwriting recognition. Therefore, quick parameter search is crucial when adapting RC to a new task.

Another case when dynamical parameters optimization is essential is testing new RC substrates when there is no prior RC parameter estimate. This becomes even more relevant when choosing between several alternative dynamical RC systems that differ in materials. For example, performing speech recognition in a bucket as in [36], which liquid is more suitable? A mixture, if then in which proportions, at which temperature, how deep would be an optimal reservoir?

As illustrated, one typically deals with multi-dimensional hyperparameter optimization. There are two quite contrary approaches towards RC hyperparameter optimization which are currently prevailing. One is a so-called hyperparameter fine-tuning (essentially, trial and error) method. Here, one relies on often partially heuristic arguments why a certain set of starting hyperparameters might be well suited. From that point one searches for the nearest, potentially only local, performance optimum. Although this ad-hoc practice can be frequently observed in the ML community, it does not guarantee an optimal hyperparameter combination.

An opposite case is a more systematic optimization approach, the grid search (GS) technique. The method consists in an exhaustive search of all hyperparameter combinations under certain constraints. GS has its advantage in guaranteeing the identification of a global hyperparameter optimum, provided that the parameter search grid is sufficiently dense. In addition, the technique provides a multidimensional error landscape, giving insight into the structure of the parameter space and through that potentially into the relationship between task and computing system. However, GS may take substantial optimization time due to the exponentially increasing amount of data points with each additional optimized hyperparameter. Therefore, in practice GS is often limited to three-four scanned hyperparameters. As a result, a high number of optimized hyperparameters in modern ML applications renders GS utilization inefficient or even virtually impossible.

In the present work, we provide a strategy how to create a data-driven self-adapting reservoir dynamics by employing an evolutionary selection-inspired technique known as genetic algorithm (GA) [37]. The GA optimization method can be regarded as a sweet spot between the two optimization extrema: it provides a systematic search while dramatically reducing the number of trials, making GA especially suitable for RC hardware design. The algorithm works with a population of *chromosomes* encoding RC dynamics properties and thereby, works with a population of RC models. The evolutionary process is achieved by applying so-called *genetic operators* recombining the information in chromosomes. Every population is evaluated so that the most fit chromosomes,

i.e. describing the most useful reservoir dynamics, tend to survive and reproduce, leading therefore to a better average configuration in every new population. Comparing to classical optimization methods such as gradient descent, (1) GAs tend to operate on encodings, not the actual parameter values, (2) GAs can handle problems with both continuous and discrete search spaces, and (3) at no additional computational cost GAs produce several alternative configurations to choose from.

II. METHODS

A. Reservoir computing

Prior to the reservoir transformation (Fig. 1), each input data matrix \mathbf{M}^c , consisting of L input feature vectors $\mathbf{c}(n), n = 1 \dots L$, is first masked by multiplying an input mask \mathbf{W}_2^I and then, temporally encoded:

$$\begin{aligned} \mathbf{W}_2^I \mathbf{c}(n) &= \mathbf{W}_2^I (c_1(n), c_2(n), \dots, c_M(n)) \\ &= (u_1(n), u_2(n), \dots, u_N(n)) \\ &= (u(t + \theta), u(t + 2\theta), \dots, u(t + N\theta)), \end{aligned} \quad (1)$$

where M is the input data dimensionality, and N is the reservoir network size. \mathbf{W}_2^I is calculated from Eq. (5) with $\mathbf{W}^I \in \mathbb{R}^{N \times M}$, ($N > M$) having weights randomly drawn from $\{-0.4; 0; 0.4\}$ (30% connectivity) and remaining fixed for all experiments. Finally, the temporally-encoded input signal $u(t)$ is kept constant in-between times $(t + i\theta, t + (i + 1)\theta)$, $i = 1 \dots N$, corresponding to the temporal separation between the virtual nodes [8]. This temporal encoding technique is sometimes called a *sample-and-hold* operation.

The temporal information input signal $u(t)$ is subsequently processed by the delayed-feedback nonlinear system reservoir (Eq. (2)). The choice of this particular reservoir dynamics model was motivated by its recent implementation as a substrate for numerous photonic RC devices [8, 17, 20], and can often be described by the low-pass delay-differential equation

$$\tau \dot{x}(t) = -x(t) + f(x(t - \tau_D) + \rho u(t)). \quad (2)$$

In our case, we employ $f(x) = \beta \sin^2(x + \Phi_0)$ as nonlinearity. The nonlinear dynamics parameters τ , β , Φ_0 , and ρ are subject to optimization while delay time $\tau_D = 6$ is kept constant in our experiments. Moreover, similar bandpass-filtered systems can be easily implemented in electro-optical substrates [38].

The result of RC $\mathbf{y}(n)$ is computed as:

$$\mathbf{y}(n) = \mathbf{W}^R \mathbf{x}(n), \quad (3)$$

where vector $\mathbf{x}(n) = (x(t + \theta), x(t + 2\theta), \dots, x(t + N\theta))$ is the decoded nonlinear reservoir response (Eq. 2). The linear readout weights \mathbf{W}^R are obtained on a computer

from previously processed data samples (Eqs (1)-(2)) using the ridge regression:

$$\mathbf{W}^R = (\mathbf{M}_x \cdot \mathbf{M}_x^T + \lambda \cdot \mathbf{I})^{-1}(\mathbf{M}_x \cdot \mathbf{T}^T), \quad (4)$$

where $\lambda \ll 1$ is a small regularization constant. $\mathbf{M}_x \in \mathbb{R}^{N \times Q}$ is a feature matrix of concatenated horizontally state vectors $\mathbf{x}(n)$. $\mathbf{T} \in \mathbb{R}^{K \times Q}$ is a teacher matrix, Q denotes output dimensionality, and K the number of training feature vectors. For classification tasks, the teacher is a *one-hot encoded* matrix, i.e. consists of target answer vectors $\mathbf{y}^{\text{tgt}} \in \mathbb{R}^{K \times 1}$ where the only nonzero elements correspond to the correct class label.

B. Enhanced masking via PCA

In our approach, we adapt the input mask to the data structure particular to each task. A new input matrix \mathbf{W}_2^I is constructed as a superposition of three linear operators, compression \mathbf{W}_c , decompression \mathbf{W}_c^T , and conventional (random) masking \mathbf{W}^I :

$$\mathbf{W}_2^I = \mathbf{W}^I \cdot \mathbf{W}_c^T \cdot \mathbf{W}_c, \quad (5)$$

where the transposed matrix pair \mathbf{W}_c and \mathbf{W}_c^T is calculated using the standard unsupervised dimensionality reduction technique of principal component analysis [39, 40]; \mathbf{W}^I is randomly generated as usual for RC. The resulting mask \mathbf{W}_2^I remains fixed during all RC experiments for the given task. Furthermore, as it optimizes input information content, it is not optimized for a particular set of dynamical reservoir dynamics.

Principal component analysis (PCA) can be described as follows. First, an isolated subset of data is selected such that it reflects the data distribution of the whole dataset. Then, a covariance matrix $\mathbf{\Sigma} \in \mathbb{R}^{M \times P_0}$ is constructed using said subset. Here, M is the input dimensionality and P_0 is the total number of feature vectors in the subset. During the next step, a new matrix $\mathbf{W} \in \mathbb{R}^{M \times M}$ is obtained such that columns in \mathbf{W} are eigenvectors of $\mathbf{\Sigma}$ sorted by decreasing magnitude of corresponding eigenvalues. This is achieved via *singular value decomposition*. Finally, a compression matrix $\mathbf{W}_c \in \mathbb{R}^{M' \times M}$ is constructed by selecting the first $M' < M$ vector-columns of \mathbf{W} , the principal components, and transposing the resulting matrix.

The superposition of compression \mathbf{W}_c and decompression \mathbf{W}_c^T operators is an autoencoder. The autoencoder $\mathbf{W}_c^T \cdot \mathbf{W}_c$ facilitates general data structure extraction by learning the most relevant features, while \mathbf{W}^I helps to map the input data onto a higher dimensional state space. Therefore, the new operator \mathbf{W}_2^I can be interpreted as a mask made more sensitive to the most relevant features in the input data, rather than the commonly employed simple random feature mapping via \mathbf{W}^I .

Another implication for ML hardware implementation of our architecture is tackling the input bottleneck. By decomposing \mathbf{W}_2^I into two independent steps, first compression \mathbf{W}_c and second masking and decompression $\mathbf{W}^I \cdot \mathbf{W}_c^T$, both steps can be performed by different units. One can therefore preprocess the information by a simplistic special unit according to the first step. The information ultimately to be injected into the physical reservoir is then compressed at ratio M/M' .

C. Hyperparameter self-optimization

Introduced in [41], genetic algorithms (GAs) are a family of evolutionary-inspired techniques based on the idea of survival of the fittest. Genetic algorithms can be generally described as follows:

Algorithm 1.

```

Random initial population
repeat
    Fitness evaluation
    Selection
    Crossover and mutation
until Converged

```

First, an initial random population of chromosomes is generated. This stage corresponds to a completely random search. Then, each chromosome is evaluated according to a certain loss function. The objective of the optimization is to minimize the loss function, therefore the most fit are individuals with the lowest error score. The most fit individuals are more likely to be selected for reproduction. Finally, application of genetic operators of *crossover* and *mutation* over selected chromosomes results in a new population of chromosomes with improved average fitness. The process is repeated until convergence or for a fixed number of iterations. Note that GAs use probabilistic computations and each realization may lead to a different result. Below, we provide more details specific to our particular GA implementation [42].

Hyperparameters encoding

A chromosome represents a unique hyperparameters configuration, and therefore encodes all optimized hyperparameter values. Here, we restrain ourselves to optimize only RC dynamics parameters, however, any other hyperparameters, such as for example the number of principal components, could be potentially encoded in a chromosome. To describe the encoded parameter values, we utilize a binary encoding. The advantage of this scheme is a straightforward implementation of genetic operators. The shortcoming is an always finite resolution of parameters encoded in chromosomes. Note that this shortcoming is not relevant to physical RC realizations since physical systems usually do not allow very precise dynamical parameters tuning.

| GA meta-parameter | Value |
|-------------------------------------|-------|
| Crossover rate, r_c | 88% |
| Mutation rate, r_m | 12% |
| Crossover prob. (uniform crossover) | 50% |
| Bit mutation prob., p_u | 20% |
| Population size, N_{pop} | 20 |
| Archive size, N_{ar} | 12 |
| Total no. of generations | 40 |

Table I. Summary of GA parameters. Total no. of RC training: $40 \times 20 = 800$ evaluations.

For the sake of illustration let us decode a 10 bit binary chromosome $\langle 11.000|00.110 \rangle$. In this example, the values are represented as signed 5 bit fixed-point numbers with a 3 bit fractional part. For convenience, we have separated the values with a '|' and fractional parts with a '.'. Hence we see that there are two values encoded with the resolution of 2^{-3} . Minimal and maximal possible encoded values are -2 and 1.875 . By convention, the first (sign) bit signifies the maximal power of two with a negative value, here it is -2^1 . The subsequent bits have positive values and correspond to powers 2^0 , 2^{-1} , 2^{-2} , and 2^{-3} , respectively. Therefore, the first encoded value $\langle 11.000 \rangle = -2^1 \cdot 1 + 2^0 \cdot 1 + 2^{-1} \cdot 0 + 2^{-2} \cdot 0 + 2^{-3} \cdot 0 = -1$. The second value $\langle 00.110 \rangle = -2^1 \cdot 0 + 2^0 \cdot 0 + 2^{-1} \cdot 1 + 2^{-2} \cdot 1 + 2^{-3} \cdot 0 = 0.75$. Note that we vary parameter ranges and bit resolutions between actual parameter values (see Table II).

Fitness evaluation and reproduction

Before genetic operators can be applied, the chromosomes in population have to be evaluated against a certain loss function. Therefore, an N_{pop} (see Table I) number of RC systems are trained with dynamics parameters encoded in corresponding chromosomes. RC systems are then evaluated on an isolated validation dataset. This allows us to assign losses in terms of word error rates.

A tournament selection is applied when selecting parent chromosomes for reproduction. The selection is performed using genetic material from current population with N_{pop} members and a certain number of the fittest chromosomes ("archive") N_{ar} from the previous population. Therefore, the total number of chromosomes for tournament selection is $N_{pop} + N_{ar}$. The selection mechanism first randomly chooses two chromosomes. Then, only the chromosome with the smaller loss (a tournament "winner") is selected as a parent. The crossover operator is binary and therefore requires two parents, i.e. two tournaments are performed before a crossover. Whereas only a single parent is needed for mutation. Naturally, the same chromosome may take part in several tournaments.

The crossover operator recombines information contained in all selected parent chromosome pairs and $\lfloor r_c \cdot N_{pop} \rfloor$ new chromosomes are created. Here, $\lfloor \cdot \rfloor$ denotes

"nearest integer" (rounding). A child chromosome is generated by taking each bit with the probability of 50% from the first parent or from the second parent otherwise. In the literature this is called a *uniform crossover* operator which is inspired by the chromosomal crossover in biological cells.

Mutation creates $\lfloor r_m \cdot N_{pop} \rfloor$ new chromosomes. During mutation, each chromosome bit is flipped with the probability p_u . It is crucial to balance mutation rate r_m and mutation probability p_u . If they are too high, the obtained information so far may not have been used properly. If too small, the algorithm may converge prematurely.

D. Hardware implementation

FPGA was chosen as an experimental platform for RC hardware development due to several reasons. First of all, FPGAs are well controllable and re-programmable. Second, by leveraging reservoir computing, FPGAs allow for a real-time prediction at MHz rate [43, 44]. Third, existing FPGA design may be ported to even faster electronic hardware such as application specific integrated circuits (ASICs). We decided to implement asynchronous communication between FPGA and external world, as well as between FPGA modules. A three wire communication protocol was implemented [43]. This should facilitate applications where data are coming asynchronously, such as communication with remote devices in a larger network. Moreover, having a common asynchronous communication protocol improves composition modularity and, as a result, facilitates isolated module verification. We investigate time-delay reservoirs since combining both space and time multiplexing, i.e. having multiple physical nodes with delays, has potential implementing extremely high-dimensional reservoirs [44].

We employ an Artix-7 (XC7A100T) FPGA chip as a digital hardware substrate for RC. The major part of hardware design is done in a hardware-synthesizable subset of Haskell language known as Clash project [45]. This hardware design approach achieves two goals: First, both hardware (FPGA) and software (RC simulation) have a shared environment. Certain pieces of code such as the Heun's integration scheme implementing Eq. (2) are simply reused by the FPGA design. Second, the high-level functional language drastically simplifies the hardware design and verification workflow. Clash compiles the design into a low-level VHDL hardware description language. Finally, Vivado Design Suite generates the bitstream which directly configures the FPGA.

The implemented architecture (Fig. 2) is a pipeline of three components working in parallel: masking, delayed-feedback dynamics, and readout. First, the information input is compressed on a computer using matrix \mathbf{W}_c pre-calculated via PCA. The resulting data are transferred to the FPGA via a USB cable using the serial UART protocol. The information input block is implemented

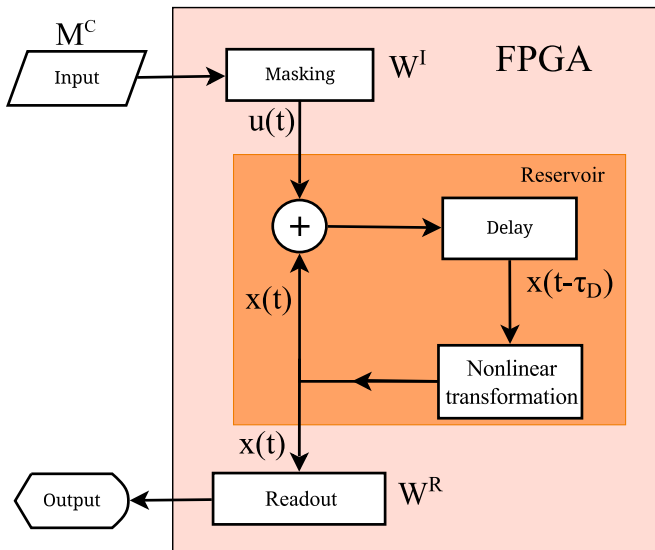


Figure 2. **FPGA-based standalone RC architecture** implements all essential RC blocks: masking, reservoir, and readout (cf. Fig. 1). Arrows represent 16+2 bit wide asynchronous communication buses.

on FPGA and fuses both masking and decompression $\mathbf{W}^I \cdot \mathbf{W}_c^T$ as a single matrix-vector multiplication operation. The matrix-vector multiplication is real-time, i.e. the component is instantly available after previous vector has been input, and is based on MAC (multiply-and-accumulate) circuits conforming to the asynchronous communication protocol. The data are then transferred to the reservoir block which simulates the delay dynamics of Eq. (2) using the second-order Heun’s method.

The FPGA implements the 16-bit fixed-point arithmetic, thus introducing quantization (digitization) noise. The impact of quantization noise could be strongly reduced by an implementation based on a floating-point module. However, the downsides of the floating-point FPGA implementation are more consumed programmable logic area and potentially slower processing rates. To demonstrate the practical applicability to other RC realizations, we stick to the less accurate fixed-point representation natively supported by our hardware.

During the training step, the system is run without the readout component. The resulting dynamics is sent to a computer where the readout matrix \mathbf{W}^R is obtained with Eq. (4). During the testing step, to avoid model overfitting, we utilize a separate testing dataset, i.e. data neither used in FPGA training, nor in model optimization.

III. RESULTS

To benefit from the underlying recurrent network, we apply RC to a time-dependent signal, human speech. The benchmark employed in this paper is a speech recognition task based on the clean isolated digits subset of Aurora-II

| Parameter | Min value | Max value | Resolution step |
|-----------|---------------------|-----------|-----------------|
| τ | $7.8 \cdot 10^{-3}$ | 0.99 | 2^{-7} |
| β | -4 | 3.98 | 2^{-6} |
| Φ_0 | 0 | π | 2^{-6} |
| ρ | -4 | 3.88 | 2^{-3} |

Table II. Parameter ranges used for GA search

database [46] (2412 samples). Following the established speech recognition paradigm, we model the dynamics of the inner ear and utilize Lyon model *cochleagrams* [47] as 64-dimensional inputs to the reservoir described by Eqs (1)-(2).

We start our experimentation with unoptimized reservoir dynamics parameters and perform GA search. Table II summarizes parameter ranges selected with respect to *physically meaningful* RC dynamics. For instance, the delay system Eq. (2) is π -periodic because of the nonlinear function $f(x) = \sin^2(x)$, therefore we restrict $\Phi_0 \in [0; \pi]$; parameter τ cannot be large with respect to delay time τ_D , otherwise the system’s complexity is substantially reduced; finally, β and ρ cannot be large otherwise the system will bifurcate away from useful dynamics. Otherwise, we do not provide any knowledge common to RC implementations (such as edge-of chaos), i.e. dynamics parameters are self-adapted to the speech recognition task.

To evaluate the classification accuracy during GA and GS optimizations, a so-called two-fold cross-validation is employed. First, training is performed on a group of 500 digits and another group of 500 digits is used for validation. Then, the roles are reversed, i.e. training is performed on the second group and validation, on the first one. Finally, a separate dataset of 1000 digits is used for testing the FPGA implementation. The remaining 412 samples are employed for PCA. Each individual step involved in our procedure is therefore carried out on a unique dataset, ensuring that findings can be transferred to applications with a typical continuous stream of input data. As an error measure (loss function) we utilize word error rate (WER), i.e. the ratio between errors and total number of evaluated samples. The genetic algorithm efficiently converges to optimal dynamics settings with small evaluations number, see Fig. 3(a), orange dotted curve. The best obtained parameters are $\tau = 7 \cdot 10^{-2}$, $\beta = -1.69$, $\Phi_0 = -1.33$, $\rho = 1.5$ with $\text{WER} = 3.8\%$.

We keep the reservoir size at a moderate value of $N = 600$ nodes in order to run the experiments quickly, though our hardware could support substantially larger systems. Our current implementation occupies about 23% of FPGA area. Time-multiplexing allows increasing the reservoir dimensions by only adding more elements to the FIFO delay line, however the most of area is occupied by circuits implementing matrix multiplication (masking and readout). Therefore, we estimate that using the same FPGA model and without any additional optimization the total number of nodes can be increased

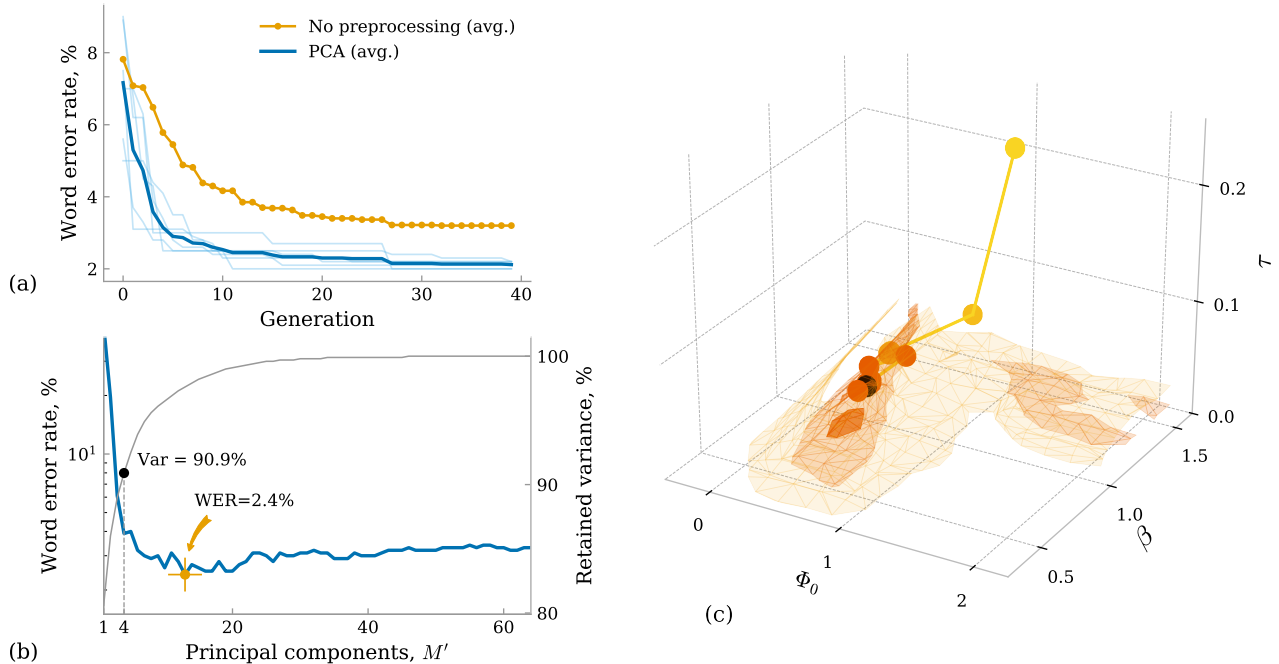


Figure 3. (a) **Genetic algorithm convergence averaged over 6 individual runs.** Individual genetic algorithm (GA) runs with PCA preprocessing are illustrated by narrow light-blue lines. The PCA preprocessing not only provides better accuracy (bold blue line) but also faster GA convergence and better overall performance than without PCA (orange dotted). Both experiments were conducted for a network of $N = 600$ virtual neurons. (b) **Selecting the number of principal components.** Principal component analysis predicts four as the minimal principal components number for current dataset. That corresponds to the retained variance of 90.9%. The most accurate value $WER = 2.4\%$ is achieved at 13 principal components (orange crosshair) with 97.6% retained variance. The small number of principal components ($M' = 13$) compared to the original number of channels ($M = 64$) indicates that the space containing human speech is sparse. Fixed (suboptimal) dynamical parameters are $\tau = 5 \cdot 10^{-3}$, $\tau_D = 6$, $\beta = 0.8$, $\Phi_0 = 0.3$, $\rho = 1.5$ (Eq. (2)). (c) **Projection of multidimensional error surfaces in 3D parameter space.** The fixed parameter is $\rho = 1.5$. The error landscape in the three parameter dimensions (Φ_0 , β , τ) is characterized by extensive grid search (11,340 data points). An example evolution of the best chromosomes in each GA generation is visualized with circles converging to a local error minimum after ~ 20 generations. The final parameter obtained by this GA run is $WER = 2.5\%$ marked in black color. The nested error isosurfaces correspond to $WER = 10, 5, 3\%$, respectively. The darkest orange volume contains the absolute error minimum of $WER = 1.9\%$.

up to 2500-2600 nodes. This number, however, can be further enlarged in several orthogonal ways: (1) by using a more powerful FPGA, which are readily available, (2) by optimizing the hardware description code and reformulating the design directly in a lower level language such as VHDL, (3) by even better adapting the RC concept to existing digital hardware.

In the next step, we study the impact of dimensionality reduction on the classification accuracy. With the help of PCA, we decrease the number of input dimensions by removing the principal components corresponding to the smallest eigenvalue magnitudes, i.e. containing the redundant information. General practice in PCA is to reduce the number of principal components so that at least 90% of variance is preserved. Therefore, we anticipate that the minimal number of principal components that can be used with these data is four (90.9% variance). This hypothesis is confirmed in Fig. 3(b), where the error sharply increases when the number of principal components goes below four. Principal component anal-

ysis shows that the best result in Fig. 3(b) is obtained for 13 principal components (97.6% of variance). Thus, we may conclude that the remaining $64 - 13 = 51$ principal components carry 2.4% of non-essential information such as noise. By removing those principal components we are able to effectively filter the residual information, which improves the recognition accuracy (Fig. 3(b)). In the rest of our experiments we reduce the number of input dimensions to seven principal components, preserving thus 94.9% of variance. That corresponds to $64/7 \simeq 9$ times compression rate. In our case, where data transfer is serial, this compression rate substantially reduces the transmission time to FPGA processing unit. Furthermore, read-only memory capacity, containing coefficients for the input masking, is reduced 9 times comparing to conventional masking without compression. Crucially, according to Fig. 3(b), recognition performance is hardly affected by this stronger compression.

The selected dimensionality reduction consistently improves the overall accuracy (Fig. 3(a), thick blue curve).

The parameters obtained by the GA $\tau = 7.8125 \cdot 10^{-3}$, $\tau_D = 6$, $\beta = -1.09375$, $\Phi_0 = -3.3125$, $\rho = 1.5$ result in an optimal performance of WER = 2.1%. Moreover, PCA preprocessing also helps the GA to converge faster. This can be explained by the fact that the space of sounds (and therefore, cochleagrams) is sparse with respect to the words pronounced by humans, hence the majority of the sound space is populated by information only weakly correlated to the information content. Therefore, a significant part of information contained in cochleagrams is redundant.

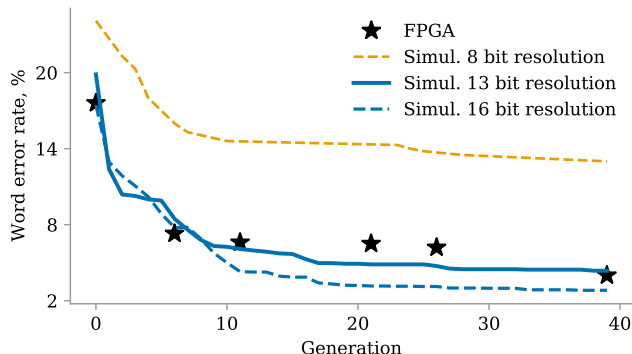


Figure 4. **Genetic algorithm convergence in hardware.** Simulation with noise averaged over 6 runs (lines) and FPGA realizations (stars). The solid line corresponds to simulation with amount of noise equal to the one in FPGA.

To better illustrate the GA search (case of PCA preprocessing), we perform grid search (GS) along the three most significant parameter dimensions, i.e. Φ_0 , β , and τ , crucially forced to use much coarser resolution: less than 25 points per dimension already result in a total of 11,340 points in parameter space. The exhaustive GS in all four parameter dimensions with resolution comparable to the one we used in GA would take 5,106 times longer than GA. If, as here for our case, a single GA run in our implementation takes around an hour, GS would take more than seven months. Adding an additional (fifth) parameter dimension scanned along e.g. 100 points, would immediately increase the GS time to 59 years. Both GA and GS can be parallelized, but in case of GS, parallelization cannot overcome the exponential growth of necessary resources. That clearly highlights the advantage of GA over exhaustive GS.

Figure 3(c) reveals error isosurfaces in the three-dimensional parameter space obtained as a result of GS. The isosurfaces present nested objects corresponding to WERs = 10%, 5%, and 3%. Error rates obtained from the GA search are visualized with circles. It can be seen that the topmost circle is a result of the random search (zero generation), corresponding to WER \simeq 16%. Then, as GA is efficiently converging, the circles are quickly approaching an acceptable local minimum. Although Fig. 3(c) illustrates the GA search in only three dimensions, GA is simultaneously optimizing parameters in all four

dimensions.

Finally, we apply the GA technique to an FPGA-based RC. Before we actually implement RC on FPGA, we accurately estimate an optimal parameter set offline on a computer. In order to take into account the quantization noise in FPGA with limited bit resolution, we simulate the limited bit resolution in Eq. (2) corresponding to the white noise of level $2^{-13} \simeq 1.2 \cdot 10^{-4}$. The noise is applied to the dynamical variable $x(t)$, the delay term $x(t - \tau_D)$, and the result of nonlinear transformation f . Additionally, to better model the behavior of our hardware, in the beginning of numerical experiment we add the noise of the same magnitude to masking coefficients and also we repeat the procedure with readout coefficients right after training.

Figure 4 shows the corresponding to FPGA 13 bit quantization noise results simulated on a computer (solid line). To highlight the impact of quantization noise, we also provide simulations for 8 bit (dashed orange curve) and 16 bit (dashed blue curve) resolutions. Due to the noise in the experiment, the accuracy of classification degrades overall. We see that for the lowest, 8 bit resolution, the accuracy is significantly deteriorated. We then select parameters from a GA optimization under simulated quantization noise of 13 bits. These parameters are then used for the RC implementation in the FPGA. Computational results obtained fully autonomously by the FPGA correspond to the black stars. They excellently match the average convergence obtained from the offline model, thereby validating our approach.

IV. CONCLUSION

We have proposed a technique towards practical application of reservoir computing (RC). The technique consists of two components: data-driven input mask optimization and efficient dynamical parameter optimization in terms of RC evaluations number. We have illustrated those methods and their strong positive impact on the speech recognition. The advanced input masking reduced the input data to be transferred to the device by 9 times and lowered the average classification error by 1.7%, a 1.8 fold improvement. The improved parameter optimization reduced the number of iterative optimization steps by 5,106 times when compared to exhaustive grid search.

We took advantage of the fact that the exact RC model was known in advance and were able to run genetic algorithm (GA) optimizations offline on a PC. We took into account the hardware's quantization noise and have illustrated the significance of its impact in possible real-world scenario. Finally, we have built an FPGA RC confirming our evolutionary technique. This illustrates how our method can be applied to various physically existing RC systems where noise is inevitably present.

Another significant benefit of GA is that the method could be applied even when the exact model of the optimized system was unknown. This would enable RC

optimization online, i.e. directly on the actual hardware, as it was done e.g. in [48]. In this work we have shown that evolutionary-inspired optimization can significantly reduce the time to adapt RC dynamics to an unforeseen task. We leave the implementation of online GA to the future investigations as the next logical step towards self-

adapting hardware [49].

ACKNOWLEDGMENTS

This work was supported by the Labex ACTION program (Contract No. ANR-11-LABX-0001-01) and by the BiPhoProc ANR project (ANR-14-OHRI-0002-02).

-
- [1] Y. LeCun, Y. Bengio, and G. E. Hinton, *Nature* **521**, 436 (2015).
- [2] B. Amos, B. Ludwiczuk, and M. Satyanarayanan, *Open-Face: A general-purpose face recognition library with mobile applications*, Tech. Rep. (CMU-CS-16-118, CMU School of Computer Science, 2016).
- [3] A. Graves, A. Mohamed, and G. Hinton, *Icassp*, 6645 (2013).
- [4] D. D. Johnson, in *Lecture Notes in Computer Science (including subseries Lecture Notes in Artificial Intelligence and Lecture Notes in Bioinformatics)*, Vol. 10198 LNCS (2017) pp. 128–143.
- [5] D. D. Johnson, R. M. Keller, and N. Weintraut, Eighth International Conference on Computational Creativity (ICCC'17), 151 (2017).
- [6] D. Silver, J. Schrittwieser, K. Simonyan, I. Antonoglou, A. Huang, A. Guez, T. Hubert, L. Baker, M. Lai, A. Bolton, Y. Chen, T. Lillicrap, F. Hui, and L. Sifre, *Nature Publishing Group* **550**, 354 (2017).
- [7] D. Silver, T. Hubert, J. Schrittwieser, I. Antonoglou, M. Lai, A. Guez, M. Lanctot, L. Sifre, D. Kumaran, T. Graepel, T. Lillicrap, K. Simonyan, and D. Hassabis, , 1 (2017).
- [8] L. Appeltant, M. C. Soriano, G. V. D. Sande, J. Danckaert, S. Massar, J. Dambre, B. Schrauwen, C. R. Mirasso, and I. Fischer, *Nature Communications* **2**, 466 (2011).
- [9] J. Torresen, *Field Programmable Logic and Application*, 1 (2004).
- [10] H. Jaeger, German National Research Center for Information Technology GMD Technical Report **148:34** (2001).
- [11] J. Steil, in *2004 IEEE International Joint Conference on Neural Networks (IEEE Cat. No.04CH37541)*, Vol. 2 (IEEE, 2004) pp. 843–848.
- [12] W. Maass, T. Natschläger, and H. Markram, *Neural Comput* **14**, 2531 (2002).
- [13] M. Hermans and B. Schrauwen, *Neural Computation* **24**, 104 (2011).
- [14] M. C. Soriano, S. Ortin, L. Keuninckx, L. Appeltant, J. Danckaert, L. Pesquera, and G. der Sande, *IEEE TRANSACTIONS ON NEURAL NETWORKS AND LEARNING SYSTEMS* **26**, 388 (2015).
- [15] L. Larger, M. C. Soriano, D. Brunner, L. Appeltant, J. M. Gutierrez, L. Pesquera, C. R. Mirasso, and I. Fischer, *Optics express* **20**, 3241 (2012).
- [16] F. Duport, B. Schneider, A. Smerieri, M. Haelterman, and S. Massar, *Optics Express* **20**, 22783 (2012).
- [17] D. Brunner, M. C. Soriano, C. R. Mirasso, and I. Fischer, *Nature Communications* **4**, 1364 (2013).
- [18] K. Vandoorne, P. Mechet, T. Van Vaerenbergh, M. Fiers, G. Morthier, D. Verstraeten, B. Schrauwen, J. Dambre, and P. Bienstman, *Nature communications* **5**, 3541 (2014).
- [19] J. Torrejon, M. Riou, F. A. Araujo, S. Tsunegi, G. Khalsa, D. Querlioz, P. Bortolotti, V. Cros, K. Yakushiji, A. Fukushima, H. Kubota, S. Yuasa, M. D. Stiles, and J. Grollier, *Nature* **547**, 428 (2017).
- [20] L. Larger, A. Baylón-Fuentes, R. Martinenghi, V. S. Udaltsov, Y. K. Chembo, and M. Jacquot, *Physical Review X* **7**, 011015 (2017).
- [21] H. Jaeger, *Science* **304**, 78 (2004).
- [22] M. C. Soriano, J. García-Ojalvo, C. R. Mirasso, and I. Fischer, *Reviews of Modern Physics* **85**, 421 (2013).
- [23] L. Larger, B. Penkovsky, and Y. Maistrenko, *Physical Review Letters* **111**, 054103 (2013).
- [24] P. Antonik, F. Duport, M. Hermans, A. Smerieri, M. Haelterman, and S. Massar, *IEEE Transactions on Neural Networks and Learning Systems* **28**, 2686 (2017).
- [25] R. Martinenghi, F. Xiaole, M. Jacquot, Y. K. Chembo, and L. Larger, **2531**, 25030 (2012).
- [26] M. Hermans, J. Dambre, and P. Bienstman, *IEEE Transactions on Neural Networks and Learning Systems* **26**, 1545 (2015).
- [27] A. Argyris, J. Bueno, and I. Fischer, *Scientific Reports* (2018), 10.1038/s41598-018-26927-y.
- [28] By hyperparameters we mean those parameters which are set before the learning begins.
- [29] J. Yperman and T. Becker, (2016).
- [30] A. A. Ferreira and T. B. Ludermit, in *2009 International Joint Conference on Neural Networks (IEEE, 2009)* pp. 811–815.
- [31] M. Rigamonti, P. Baraldi, E. Zio, I. Roychoudhury, K. Goebel, and S. Poll, in *EUROPEAN CONFERENCE OF THE PROGNOSTICS AND HEALTH MANAGEMENT SOCIETY 2016* (2016).
- [32] J. Schumacher, H. Toutounji, and G. Pipa, in *Artificial Neural Networks*, Vol. 4, edited by K. N. Koprinkova-Hristova P., Mladenov V. (Springer, Cham, 2015) artificial ed., pp. 63–90.
- [33] R. Miikkulainen, J. A. Bednar, Y. Choe, and J. Sirosh, *Psychology of Learning and Motivation - Advances in Research and Theory* **36**, 257 (1997).
- [34] Linear operators are expressed as matrices. The relationship between compression and expansion (decompression) obtained after PCA is a matrix transpose operation.
- [35] C. M. Bishop, *Pattern Recognition and Machine Learning* (Springer-Verlag Berlin, Heidelberg, 2006).
- [36] C. Fernando and S. Sojakka, in *Proceedings of the 7th European Conference on Artificial Life* (2003) pp. 588–597.
- [37] K. Deb, *Sadhana* **24**, 293 (1999).

- [38] L. Larger, B. Penkovsky, and Y. Maistrenko, *Nature Communications* **6**, 7752 (2015).
- [39] K. Pearson, *The London, Edinburgh, and Dublin Philosophical Magazine and Journal of Science* **2**, 559 (1901).
- [40] H. Hotelling, *Journal of Educational Psychology* **24**, 417 (1933).
- [41] J. H. Holland, *University of Michigan Press, Ann Arbor. (2nd Edition, MIT Press, 1992.)* (1975).
- [42] The employed genetic algorithms library was <https://hackage.haskell.org/package/GA>.
- [43] B. Penkovsky, *Theory and Modeling of Complex Non-linear Delay Dynamics Applied to Neuromorphic Computing*, Ph.D. thesis, Universite de Bourgogne Franche-Comte (2017).
- [44] D. Canaday, A. Griffith, and D. Gauthier, , 1 (2018).
- [45] Clash compiler is available via <http://clash-lang.org>.
- [46] H.-G. Hirsch and D. Pearce, *Isca Itrw Asr2000* , 181 (2000).
- [47] M. Slaney, *Apple Technical Report #13* , 1 (1988).
- [48] A. Thompson, *Evolvable Systems: From Biology to Hardware* **1259**, 390 (1996).
- [49] C. Aporntewan and P. Chongstitvatana, in *Proceedings of the 2001 Congress on Evolutionary Computation (IEEE Cat. No.01TH8546)* (2001).